Prepeak and First Sharp Diffraction Peak in the Structure Factor of $(Cs_2O)_{0.14}(B_2O_3)_{0.86}$ Glass: Influence of Temperature

Giovanna D'Angelo,*,† Cristina Crupi,† Miguel Ángel González,‡ Emilia Basile,§,∥ Valeria Conti Nibali,† and Claudia Mondelli⊥

Dipartimento di Fisica, University of Messina, Salita Sperone 31, Villaggio S. Agata, 98166 Messina, Italy, Institute Laue Langevin 6, Rue Jules Horowitz, 38042 Grenoble, France, Scuola di Specializzazione in Fisica Sanitaria, Università degli Studi 'La Sapienza', Roma, Italy, Dipartimento Tecnologie e Salute, Istituto Superiore di Sanità, Roma, Italy, and CNR-INFM OGG, Institute Laue Langevin 6, Rue Jules Horowitz, 38042 Grenoble, France

Received: January 20, 2010; Revised Manuscript Received: July 13, 2010

Neutron diffraction measurements on $(Cs_2O)_{0.14}(B_2O_3)_{0.86}$ glass were performed at varying temperature over an extended range from room temperature to 800 K. It was found that, in the same Q range where the first sharp diffraction peak (FSDP) is observed in the static structure factor of almost all glass-forming systems, cesium borate glass shows two peaks. The intensities of these peaks increase with temperature, and their positions shift to lower Q values, in agreement with the peculiarities of the FSDP of network glasses. A description of this anomalous temperature dependence in terms of thermal relaxations of strained bonding arrangements of boron oxide units lying on the boundaries of cages present in the boron skeleton matrix is suggested. By comparing the diffraction patterns of a $(Cs_2O)_{0.14}(B_2O_3)_{0.86}$ sample before and after a high-temperature thermal treatment with the spectra of cesium crystals, a correspondence between the medium-range structure in the glass and the related crystalline phases has been inferred.

I. Introduction

The origin of the so-called first sharp diffraction peak (FSDP), revealed at low values of the scattering wave vector, Q ($= |Q|$) < 2 Å^{-1}, in the static structure factor, $S(Q)$, of amorphous materials, remains a central issue for unravelling the details of intermediate-range order in these systems.[1] The position ($\sim$1−1.5 Å^{-1}) of the FSDP corresponds to large real-space distances (>0.4 nm), suggesting that its origin is due to correlations extending beyond the nearest-neighbor distances, a remarkable long-range in a disordered solid. In the past few years, diffraction experiments on model binary glasses have shown that the length scale associated with the intermediate range and linked to the FSDP arises from topological ordering.[2] In addition, atomic ordering has also been found that extends to distances well beyond the domain of the FSDP and that has a periodicity given by $2\pi/Q_{PP}$, where Q_{PP} is the position of the principal peak in the measured partial structure factors. This extended length scale has been associated with the chemical atomic ordering.[2]

Understanding the mysteries of the origin of structural ordering in glasses is a fundamental step toward the comprehension of important glassy dynamic phenomena. In particular, it has been recently suggested that the mesoscopic length scale, characteristic of the intermediate-range order of glasses, plays a primary role in the low-frequency vibrational dynamics in glasses,[3] settling the breakdown of the elastic continuum approximation,[4] which, in turn, leads to the appearance of the boson peak and of the anomalous low-temperature thermal properties in glasses.[5,6]

However, despite numerous and intensive studies, many features concerning the nature of the correlations that give rise to the FSDP in relation to changes in thermodynamic parameters remain presently unsolved. For example, the FSDP exhibits an anomalous and still poorly understood behavior in its temperature dependence compared to all other peaks in $S(Q)$. In fact, its intensity increases reversibly with increasing temperature differently from what it is predicted by the Debye−Waller function.[7,8] Additionally, this peak seems to be unusually more sensitive to the application of pressure than the other features of the diffraction pattern, as its intensity decreases and its Q position shifts to higher values when pressure is increased.[9]

Several different explanations have been proposed to elucidate these anomalous characteristics of the FSDP. Among them, the idea that the FSDP arises from a quasi-Bragg reflection by quasi-lattice planes in glasses, analogous to Bragg planes in compositionally equivalent crystals,[10] has gained considerable interest owing its implied generality. This conjecture, in fact, appears to be highly appropriate for describing the presence of the FSDP not only in covalently structured glasses such as silica, but also in close-packed amorphous alloys, molecular glasses, and even melts at high temperatures.[11] In more detail, this explanation is based on the observation that, in many amorphous materials, the wave vector of the FSDP is close to the wave vector of the first strong diffraction peak of the related crystalline phase. Consequently, it is proposed that remnants of the crystalline lattice planes exist in the disordered phase and that scattering from these planes causes the FSDP.

An interesting alternative description of the origin of the FSDP is based on the existence in glasses of structural voids

* To whom correspondence should be addressed. E-mail: gdangelo@unime.it.

† University of Messina, Dipartimento di Fisica, University of Messina, Viale F. Stagno d'Alcontres 31, Villaggio S. Agata, 98166 Messina, Italy.

‡ Institute Laue Langevin 6, Rue Jules Horowitz, 38042 Grenoble, France.

§ Scuola di Specializzazione in Fisica Sanitaria, Universita degli Studi 'La Sapienza', Via Ariosto 25, 00185 Roma, Italy.

∥ Istituto Superiore di Sanita, Dipartimento Tecnologie e Salute, Viale Regina Elena, 299-00161 Roma, Italy.

⊥ CNR-INFM-OGG and CRS Soft, Institute Laue Langevin 6, Rue Jules Horowitz, 38042 Grenoble, France.

10.1021/jp1005555
Published on Web 09/15/2010

that are a distinctive structural feature of covalent glasses,[12,13] as evidenced by studies of the diffusivity of rare gases and alkalis in amorphous SiO_2, GeO_2, and B_2O_3.[14] This void-based model interprets the FSDP in glasses as a prepeak in the concentration−concentration structure factor due to the chemical ordering of interstitial voids around cation-centered clusters. Predictions of changes in the FSDP following the filling of voids with foreign atoms and of changes in the FSDP intensity following an increase in temperature or the application of pressure have also been put forward. Even though this model was proposed for covalent glasses, it can be easily employed for describing the scattering arising from low-density regions present in amorphous systems.

We believe that useful information concerning the origin and the nature of the structural correlations generating the FSDP in glasses can be obtained by directly following the structural changes that occur during the transformation from the vitreous to the crystalline phase.

Oxide glasses containing network modifiers appear to be ideal candidates for such a study, being easily transformed into polycrystals when subjected to well-controlled thermal annealing processes;[15] hence, the changes in the FSDP induced by the structural modifications that occur when the sample crystallizes can be easily studied. At the same time, these systems also offer the advantage of elucidating the role of structural voids in glasses. In fact, the presence of a metallic oxide in an oxide matrix causes the expansion of the glassy network as a result of the formation of cavities inside which network-modifying cations are arranged in proximity to nonbridging oxygen atoms, and it is supposed that the first diffraction peak in these systems reflects the periodicity resulting from holes in the network.[16]

Recently, we performed a study on low-energy vibrational dynamics in the series of alkaline borate glasses $(M_2O)_x(B_2O_3)_{1-x}$ ($M^+ = Li^+, Na^+, K^+, Cs^+$) for $x = 0.14$ by inelastic Raman and neutron scattering and low-temperature specific heat measurements.[5] We supposed that the boson peak arises from the softening of the shear modulus through the low-density defect regions that have nanometer sizes and are formed as a consequence of the dynamic arrest at the glass transition temperature. Furthermore, we found an enhanced boson peak in the cesium glass as compared to other alkaline borate glasses.

It is believed that knowledge of the intermediate structure of this system could be useful in understanding the origin of its marked low-frequency vibrational dynamics. Following this task, we performed in situ high-temperature neutron diffraction measurements on $(Cs_2O)_{0.14}(B_2O_3)_{0.86}$ glass.

In particular, in cesium borate glasses, crystallization takes place at high temperatures; for this reason, a wide range of temperatures, both below and above the glass transition, can be investigated to follow the temperature dependence of the FSDP in the amorphous phase.

II. Experimental Details

Sample Preparation. $(Cs_2O)_{0.14}(B_2O_3)_{0.86}$ glass was prepared from laboratory-reagent 99.99% purity grades of cesium nitrate and boron oxide with a stated ^{11}B enrichment of 99% in order to minimize the influence of the high neutron absorption of the ^{10}B present in natural boron. The mixed powders, whose total quantity was about 20 g, were melted in a crucible within an electric furnace by heating to 1373 K at a rate of 1 K/s. The mixture was kept at 1373 K for more than 6 h and occasionally stirred to ensure homogeneity of the liquid, and then the melt was cast into a mold.

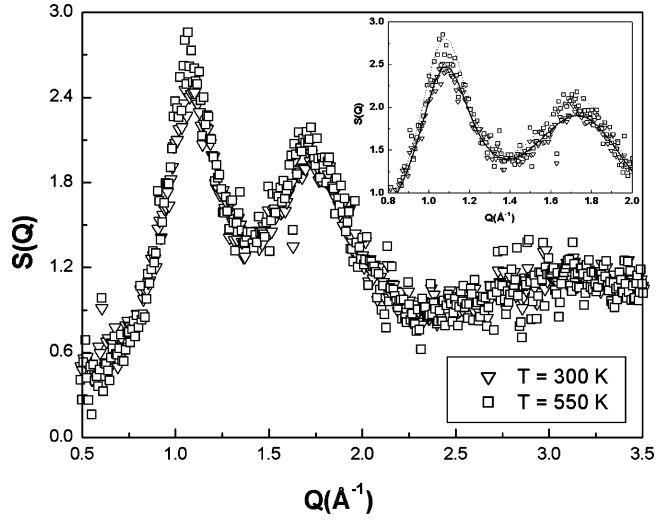

Figure 1. Temperature dependence of the static structure factor of $(Cs_2O)_{0.14}(B_2O_3)_{0.86}$ at $T = (\triangledown)$ 300 and $(\square)$ 550 K. Inset: Enlargement of the most striking changes induced by temperature in the low-Q region of the structure factors. The dotted and continuous lines indicate the Gaussian curves fitting the experimental data.

An X-ray diffraction measurement revealed a pattern with no crystalline peaks, confirming the amorphous nature of the sample. A T_g value of 550 K for the sample was determined by a thermogram measured on a Perkin-Elmer differential scanning calorimeter (DSC-Pyris) at a heating rate of 20 K/min. Afterward, the glass was annealed and stabilized at about 20 K above its calorimetric glass transition temperature in a high-purity nitrogen atmosphere and then cooled to room temperature. Finally, the sample was ground into a powder and stored in a vacuum-sealed desiccator to avoid unwanted reaction with moisture.

Neutron Measurements. Neutron diffraction experiments were performed using the D1b instrument at the Institut Laue-Langevin in Grenoble, with an incident neutron wavelength of 2.52 Å, which allowed access to a Q range of 0.5−3.4 Å^{-1}. A cylindrical vanadium can was used to contain the powdered sample and was mounted in the center of a cylindrical furnace. Diffraction patterns were acquired at different temperatures between 300 and 800 K with a step size of 50 K. Additional measurements were carried out for the empty container and for a vanadium rod with dimensions comparable to those of the sample. The data were corrected for the contributions of the background scattering from the empty vanadium can, multiple scattering, and absorption. Moreover, the data were normalized to an absolute scale with the isotropic incoherent scattering of the vanadium. Isothermal diffraction spectra at temperatures between 300 and 750 K were collected for a time of 1 h. All measurements performed at temperatures between 300 and 700 K, that is, the temperature range where the sample remains in a structurally disordered state (glass below 550 K and supercooled liquid up to 700 K), were followed by a room-temperature cycle to check for any irreversible changes arising from annealing during heating, and the same starting intensities of the two peaks were measured.

In contrast, the measurement at 800 K was taken for 24 h to ensure that the sample was in a well-balanced crystallized phase.

III. Experimental Results

The total structure factor of $(Cs_2O)_{0.14}(B_2O_3)_{0.86}$ at 300 K and $Q < 3.5$ Å^{-1} is shown in Figure 1. The most striking features

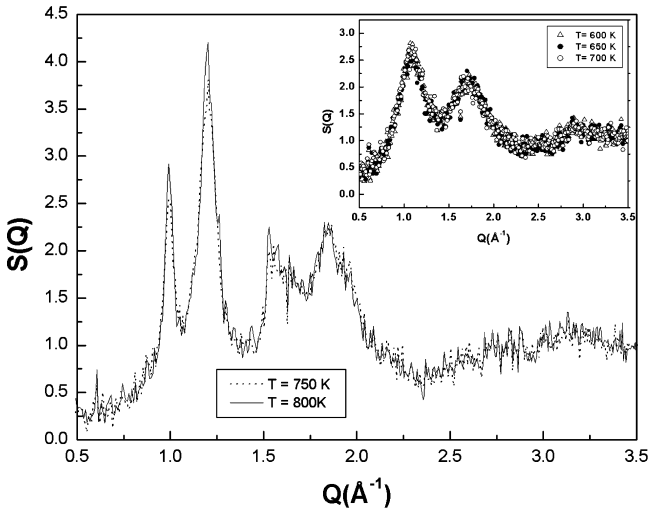

Figure 2. Static structure factor, $S(Q)$, at T = (- - -) 750 and (—) 800 K of $(Cs_2O)_{0.14}(B_2O_3)_{0.86}$ in the crystalline phase. Inset: $S(Q)$ at T = (Δ) 600, (●) 650, and (○) 700 K.

are the two intense peaks at $Q_1 = 1.06$ Å^{-1} and $Q_2 = 1.74$ Å^{-1}, although a third less intense peak is also observed in the high-Q part of the $S(Q)$ above 2.5 Å^{-1}.

Upon increasing the temperature from 300 to 550 K in steps of 50 K, gradual changes in the features of the $S(Q)$ below 2.5 Å^{-1} were observed.

In Figure 1, only the two extreme temperatures at which the changes are most evident are reported, and one can clearly observe that the intensities of the two peaks increase, with the peak at lower Q exhibiting the larger enhancement. Furthermore, both peaks shift to lower Q values, with the displacement of the second peak being greater.

In the inset in Figure 1, an enlargement of the peak regions is shown to more clearly emphasize the observed differences.

When the sample was heated above T_g, the intensities of both peaks decreased slightly (see the inset in Figure 2). Once the temperature of 750 K was achieved, drastic changes appeared. Both peaks below 2.5 Å^{-1} split into two distinct sharp spectral features, providing evidence of the onset of crystallization. Then, the temperature was set at 800 K, and 24 diffractograms of 1 h each were acquired. The increased acquisition time was considered approximately equivalent to a longer heat-treatment time for the sample. All of these diffraction patterns are nearly the same, except for a negligible change of about 2% in the intensity of the peaks below 2.5 Å^{-1} as a function of acquisition time. No differences in the Q positions of these peaks were observed. The diffraction pattern at $T = 800$ K, shown in Figure 2, was obtained by summing the 24 acquired diffractograms. It can be observed that the sum is quite similar to the diffraction pattern at 750 K, except for the small increase of the intensities of lower peaks. Moreover, the data in Figure 2 show that the crystallization is partial because, even after the annealing treatment, a significant contribution from the amorphous phase remains.

IV. Discussion

The most significant feature revealed at room temperature in the low-Q region of the structure factor of $(Cs_2O)_{0.14}(B_2O_3)_{0.86}$ is the presence of two peaks instead of the single peak at 1.61 Å^{-1} observed in the $S(Q)$ neutron pattern of B_2O_3.[17] The position of the second peak, Q_2, corresponds to a characteristic repeat distance in real space of $L_2 = 2\pi/Q_2 \approx 3.61$ Å, slightly lower than the value $L \approx 3.90$ Å similarly obtained for pure B_2O_3. On the contrary, the peak located at lower momentum transfer, Q_1, implies the existence of ordering on an extended length scale of $L_1 = 2\pi/Q_1 \approx 5.92$ Å. Furthermore, the peaks at Q_1 and Q_2 have full widths at half-maximum, ΔQ, of 0.35 and 0.72 Å^{-1}, describing degrees of ordering with coherence lengths ($l = 2\pi/\Delta Q$) of ∼18 and ∼9 Å, respectively, rather spread for the first peak.

The appearance of an extended ordered arrangement upon addition of cesium oxide to B_2O_3 is reminiscent of an analogous situation observed in inorganic network glasses, where a prepeak arises upon addition of modifier metallic oxide to vitreous silica[7,18] and germania.[19] Large changes in the low-Q range were also observed in binary borate glasses by Swenson et al.[20] after the introduction of an increasing amount of Ag_2O. They also found that the short-range order involving the first B−O, B−B, and O−O interatomic distances does not depend so much on the doping.

Modified borate glasses are based on boron oxide that is essentially built up by corner sharing of planar BO_3 triangles, many of which are grouped in planar B_3O_6 boroxol rings.[21] By adding an alkaline oxide, progressive conversion of some BO_3 triangles into tetrahedral BO_4^- units takes place, with consequent changes in the network structure including the formation of new types of anionic borate groups.[22] Metallic ions do not directly take part in the network formation[20,23] but enter the system as singly charged cations residing in the proximity of negatively charged nonbridging oxygens and BO_4^- groups in the large cages of the B−O network structure to provide local charge neutrality. Taking into account the structural characteristics of these modified borate glasses, we believe that the two lowest peaks in the static structure factor of $(Cs_2O)_{0.14}(B_2O_3)_{0.86}$ glass refer to the order of cages of different sizes formed by the topological connection of BO_3 (unfilled voids) and BO_3 and BO_4^- (voids hosting alkalis) units in the network. Voids housing cesium ions are expected to be rather wide, owing to the large size of these alkali ions. Their presence is related to the lower-Q peak, whereas the peak at higher Q refers to unfilled voids. Similar findings come from the results of molecular dynamics simulations that some of us obtained very recently.[24] In that study, the structures of the full series of alkaline borate glasses were investigated, paying attention to the role of the metallic cation in determining the intermediate-range order in these systems. With increasing alkaline ion size, a peak in the very low Q region is observed, together with a decreasing number of BO_4^- units, in reasonable agreement with the trends observed experimentally.[22] In particular, it was found that, when Cs^+ ions are added to B_2O_3, a prepeak at 1.1 Å^{-1} appears in $S(Q)$, with an intensity that increases with increasing alkali concentration to the detriment of the FSDP intensity, although its position remains unchanged. In ref 24, the observed invariance of the Q position with the molar fraction of Cs_2O (clearly visible in Figure 3 of the same work) was considered as being related to a peak arising from the same structural element for all the investigated glasses. This peak was found to arise mainly from the contributions of the B−B, the O−O, and in particular the B−O partial static structure factors (see Figure 4 of ref 24). Moreover, the analysis of the void distribution, performed using the Voronoy−Delaunay approach, revealed the existence of two characteristic correlation lengths corresponding to different sizes of the interstices present in the B−O matrix (see Figure 5b of ref 24). The increased characteristic correlation length was supposed to describe how the network rearranges to accommodate the alkaline ions and was considered to be at the origin

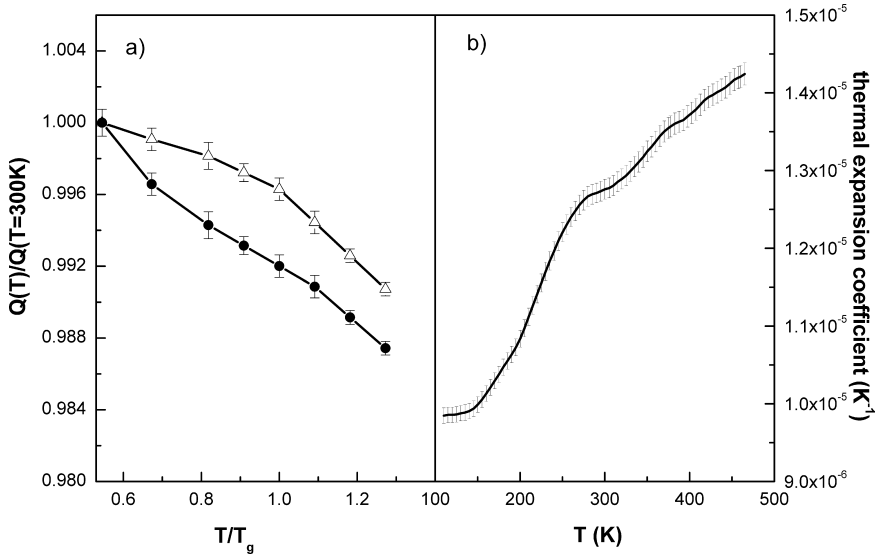

Figure 3. (a) Q position normalized to the Q value at room temperature for the (Δ) first and (●) second peaks in the diffraction patterns. (b) Mean linear thermal expansion coefficient (α_{th}) as a function of temperature.

of the appearance of the prepeak in the low-Q region of the static structure factor.

The current study reveals that, when the temperature is increased to about T_g, the two lowest peaks observed in the structure factor of $(Cs_2O)_{0.14}(B_2O_3)_{0.86}$ glass show a remarkable enhancement in their intensity and a shifting toward the low-Q side, whereas the third peak remains almost unchanged (see Figure 1).

As remarked previously, the decrease in the Q position is more pronounced for the second peak than for the first, becoming more evident above glass transition temperature, as can be observed in Figure 3a, where Q values at different temperatures normalized to the Q position at room temperature, for both peaks, are represented as a function of the reduced temperature, T/T_g. It is worth emphasizing that the observed Q decrement is indicative of an increasing repetitive characteristic distance between structural units that, therefore, space out progressively with increasing temperature. This result is clear evidence of an occurring expansion of the network involving, in particular, low-atomic-packing zones and, more importantly, unfilled voids. This finding is in agreement with the results of thermal expansion measurements on $(Cs_2O)_{0.14}(B_2O_3)_{0.86}$ glass by a pushrod horizontal dilatometer, which showed increasing values of the mean linear thermal expansion coefficient as a function of temperature (see Figure 3b).

Moreover, from the shifts of the peaks with temperature, we were able to evaluate the coefficient of linear expansion, α_p, from the equation

$$\alpha_p = \frac{1}{Q_p}\frac{dQ_p}{dT}$$

We obtained the values $\alpha_{p1} = 18.7 \times 10^{-6}$ K^{-1} and $\alpha_{p2} = 23.1 \times 10^{-6}$ K^{-1} from the temperature shifts of the first and second peaks, respectively, calculated over the range from 300 to 450 K. The corresponding experimental shifts, $\Delta Q_{p1}^{exp} = 0.003$ Å^{-1} and $\Delta Q_{p2}^{exp} = 0.006$ Å^{-1}, were obtained from the centers of Gaussian curves fitting the experimental data. The significant difference between the two thermal expansion values measured from the first and second shifts should refer to two possible different regions in the glass. The α_p values were compared with the mean linear thermal expansion coefficient $\alpha_{th} = 14.3 \times 10^{-6}$ K^{-1} at $T = 460$ K. It is worth pointing out that the expansion α_{th}, at a fixed temperature, represents an average value taking into account the elongations and contractions of all atomic distances distributed on different length scales. Otherwise, the evaluation of the shifts of diffraction peaks allows more detailed information regarding microscopic structure changes to be obtained. We found that the value of α_{th} underestimates both of the α_p expansion values obtained from diffraction, with the difference being greater for α_{p2}. A possible microscopic description of this finding is that the expansion of the glass upon heating greatly affects the structural arrangements on the intermediate length scale, whereas the structural arrangements on distances shorter than 3 Å expand much less. Moreover, because the thermal expansion is related to lattice anharmonicity, the evidence for $\alpha_{p2} > \alpha_{p1}$ indicates that the anharmonicity in the unfilled voids is larger than that in voids hosting alkalis.

Considering the shapes of the two lowest peaks, it can be observed that their sharpening is also anomalous because, as the temperature is raised, the broadening of diffraction peaks is expected as a consequence of the enhancement of thermal vibrations. On the contrary, it suggests a tendency toward a higher degree of ordering, describing an increase in the correlation lengths or a more ordered, homogeneous structure occurring at high temperature. At the same time, the intensity of the first peak increases much faster than that of the second peak, revealing that there is a greater trend toward order on one length scale and less on the other when the temperature rises. This is shown in Figure 4, where the ratios of the peak intensities $S(Q_1)$ and $S(Q_2)$ at temperature T to their corresponding intensities at room temperature are compared. The increase in the intensity with increasing temperature is quite large for the first peak, being about 9% at $T = 600$ K, whereas for the second peak, it amounts to about 3% at most.

Another atypical behavior can be observed for the region above 2.5 Å^{-1} in the diffraction pattern. In fact, the unchanging intensity of the third peak in $S(Q)$, which is associated to the short-range length scale, is also anomalous, if it is compared, for example, with the temperature dependence of the structure factor of glassy chalcogenides.[8] In fact, this peak corresponds to the second diffraction peak (the principal peak) observed in

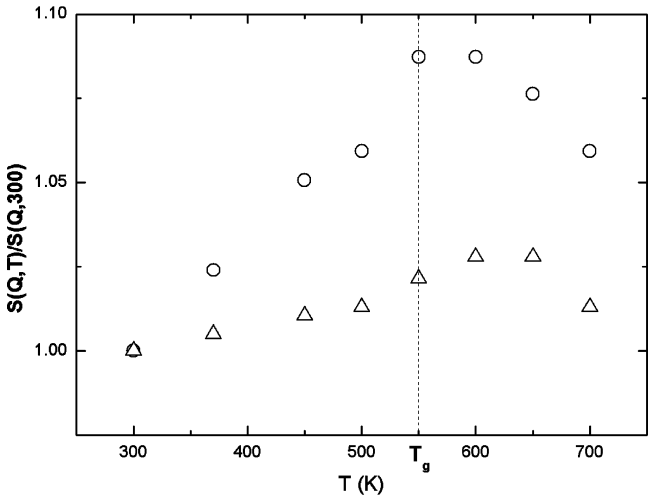

Figure 4. Ratios of the peak intensities (○) $S(Q_1)$ and (△) $S(Q_2)$ at temperature T to their corresponding intensities at room temperature. The glass transition temperature T_g is indicated by a dashed line.

the static structure factor of As_2Se_3 and As_xS_{1-x} glasses, which displays a decreasing intensity with increasing temperature.

However, it is interesting to observe that, also in potassium disilicate glass,[7] when temperature is increased, the intensity of the principal peak at about 3 $Å^{-1}$ remains unchanged, whereas changes are observed in the low-Q region of $S(Q)$. In this glass, similarly to the cesium glass, two peaks are present in the low-Q region of the diffraction pattern, instead of only one, as in pure SiO_2. However, upon increasing the temperature above the glass transition temperature, the first peak markedly increases in intensity, whereas the second peak decreases. These facts contrast with the observation of a decreased intensity of both peaks above T_g in cesium glass (see Figure 4). More importantly, during the heating steps, no sign of crystallization was observed in potassium glass, although the neutron data were collected over a long time to allow full relaxation of the structure. It appears that the cesium glass has a prevalent tendency toward crystallization, whereas the silicate one has an inclination toward the liquid state. It is believed that the presence of heavy metallic cations inside the glassy oxide matrix promotes crystallization. In fact, a similar situation is recovered in rubidium phosphate binary glass, in which an increased intensity of the FSDP with temperature and indications of crystallization near and above T_g have been found, in opposition to the behavior observed for lithium phosphate glass.[25]

Moreover, it is supposed that, in cesium borate glass, the short-range order is preserved at the temperatures investigated, because of the high rigidity of this glass,[6] whereas thermal relaxations in the intermediate-range structure are responsible for the increase in the intensities of the two lowest peaks. In particular, we believe that the increase in the intensity of the low-Q peaks with increasing temperature is due to the strengthening of the correlations between atoms placed along the edges of the cages. As the temperature rises, the strained bonding arrangements of borate units lying on the boundaries of the cages relax, making the contours of the cages more regular. More flexible bending for the B−O−B angles on the boundaries of the larger cages hosting Cs^+ cations is expected. Because of the higher flexibility, the cages can more easily relax toward more ordered configurations, strengthening the correlations between the atoms along the edges of the cages and giving rise to the observed sharper increase of the peak at 1.0 $Å^{-1}$ in the static structure factor.

Furthermore, because of their large size, cesium ions, entering the larger cages, strongly displace the oxygen atoms on their boundaries. Consequently, the cages not filled with Cs ions will be contracted, setting the position of the second diffraction peak to a Q value higher than that of the FSDP of pure boron oxide.

We also investigated the structural changes in the low-Q region occurring during the crystallization process.

A different scenario occurs when the temperature is raised above 700 K, as each of the two lowest features in the $S(Q)$ evolves in two separate strong and sharp peaks. It must be stressed that the presence of the background indicates that the system is never completely crystallized, although the appearance of several peaks denotes the incoming glass crystallization caused by increasing temperature. Moreover, despite we do not know the specific polymorphs formed by devitrification, the experimental observation of unchanged shape of the structure factor at 800 K with respect to the measurement at 750 K indicates that crystallization is going along through highly stable crystalline phases of cesium borate occurring from the beginning of heating.

We are mainly interested in the splitting of the first peak of $S(Q)$ of glass. The positions of the two new peaks are 0.99 and 1.2 $Å^{-1}$, corresponding to correlation lengths of 6.34 and 5.23 Å respectively, whereas the relative widths, ΔQ, are 0.09 and 0.12 $Å^{-1}$, describing degrees of ordering with coherence lengths longer than 70 Å. In accordance with the molecular dynamic simulation results,[24] which established that the first peak in glasses arises mainly from the contribution of the B−O and O−O partial static structure factors, we assume that these lengths correspond to two different O−O distances, setting two different sizes of the interstices present in the B−O matrix, hosting the Cs ions. The finding of alkaline cations located in distinct independent crystallographic positions is typical of binary borate crystals.[26,27] Moreover, these cations have different and irregular oxygenated environments and are located in cavities or tunnels compatible with their radius, compensating the anionic charges, just as in the corresponding glasses. Assuming that the alkaline cation sets about in the center of these spaces, the O−O distances will be related to the Cs−O lengths; consequently, it will be possible to verify how the experimental lengths match with the literature data of Cs−O distances in cesium borate crystals.

Different crystal structures of anhydrous cesium borates with ratios of metal oxide to boron oxide of less than 1 are known.[27−29] In an attempt to recognize the incoming crystalline phases that are forming during thermal annealing, the experimental $S(Q)$ was compared with the diffraction patterns of well-known cesium borate crystals obtained from the Inorganic Crystal Structure Database (ICSD). This comparison was difficult because we had a non-negligible contribution of the remaining amorphous phase and because the in situ growth of the crystals probably means that we did not have a good powder average in our sample. Therefore, the intensities of the Bragg peaks observed are not reliable, as they can be strongly influenced by texturing effects. Nevertheless, the positions of the crystalline peaks observed is not affected by any of those effects, and in the thermally treated sample, we can identify the presence of crystals of $(Cs_2O)_{0.25}(B_2O_3)_{0.75}$ (also known as cesium triborate) as the predominant phase, although the presence of crystals of $(Cs_2O)_{0.10}(B_2O_3)_{0.90}$ cannot be excluded.

The contemporaneous presence of two phases is a consequence of the complex kinetics of crystallization. In fact, crystallization of glassy borate systems containing alkalis is usually a multistage progress, owing to the limited mobility of

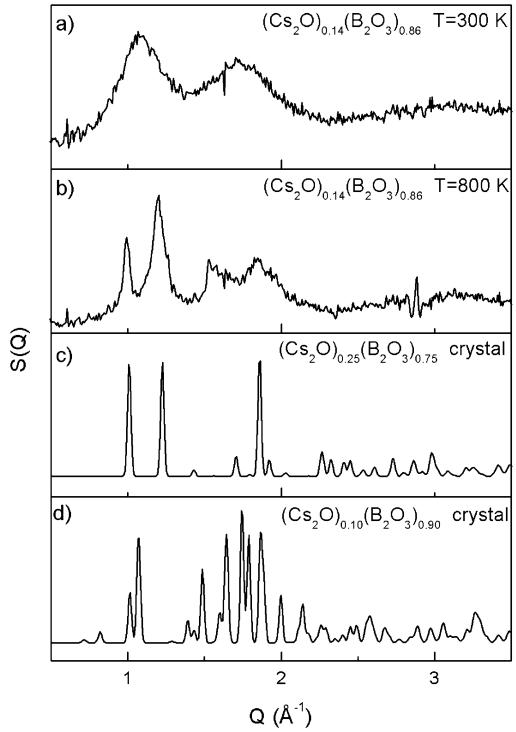

Figure 5. Comparison among the diffraction patterns at the same instrumental resolution of (a) $(Cs_2O)_{0.14}(B_2O_3)_{0.86}$ glass at $T = 300$ K, (b) $(Cs_2O)_{0.14}(B_2O_3)_{0.86}$ thermally treated at $T = 800$ K, (c) $(Cs_2O)_{0.25}(B_2O_3)_{0.75}$ crystal[26] from the ICSD, and (d) $(Cs_2O)_{0.10}(B_2O_3)_{0.90}$ crystal[25] from the ICSD.

the components in the amorphous structure of borate. With increasing temperature, different cations become displaced at smaller or greater distances depending on their diffusion coefficients, giving rise to phase segregations and eventually to the formation of several stable phases with different compositions.[30] On the other hand, $(Cs_2O)_{0.14}(B_2O_3)_{0.86}$ glass does not correspond to any of the known crystal compositions, and we believe that this starting situation can favor phase segregation.

Comparison of the diffraction pattern of the glass with those of the thermal treated and crystalline systems (shown in Figure 5) indicates that the amorphization causes most of the diffraction lines to disappear, but some of them are remodelled in diffuse bands. More importantly, some type of intermediate-range order occurs in the glassy structure, just within the same range of wavevectors in which the strongest lines of the crystalline phase are found. It is rather clear from Figure 5 that the peaks at 0.99 and 1.2 Å^{-1}, appearing in the borate system after thermal treatment, correspond to the atomic distances of structures of cesium triborate.

The borate anions in cesium triborate comprise a single three-dimensional framework. The fundamental building blocks in the anionic framework are constituted by three boron atoms. The Cs atoms occupy large cavities within the framework and do not have a well-defined coordination sphere of oxygens. If the coordination is arbitrarily taken to include all cesium−oxygen distances below 4 Å, 10 oxygens surround each cesium atom, and the Cs−O distances range from 3.967 to 3.030 Å.[29]

We assume that the two extreme Cs−O values in $(Cs_2O)_{0.25}(B_2O_3)_{0.75}$ crystal correspond to the in-plane semiprincipal axes of ellipsoidal sites of Cs^+. By comparing these values with one-half of the correlation length derived from diffraction data, equal to 3.17 and 2.61 Å, respectively, we note, at first sight, a poor agreement. However, it has to be considered that, in binary borate systems, alkaline cations occupy off-center arrangements in the cavities of borate skeleton. For example, in cesium triborate, the widest O−Cs−O bond angle for different oxygens range from 164° to 114°,[29] so that the shorter distance between two opposite atoms along the edge of the cavity compared to the real Cs−O distance can be reasonably justified. In light of this result, the lowest peak revealed in the diffraction pattern of the glassy sample can be believed as merely characterized by broadened envelopes of the corresponding peaks of crystalline phase. More precisely, whereas the crystal exhibits voids or cavities of a specific size, causing the appearance of distinct peaks, the glass is characterized by a distribution of void sizes, whose mean value corresponds to the Q position at the maximum of the single broadened peak in $S(Q)$. Obviously, the shapes of these structural voids are expected to be highly irregular and asymmetric in the glass as a consequence of the structural arrest taking place during glass formation. This implies strained bonding arrangements of borate units lying on the cage boundaries. Similar conclusions could be drawn about the peak at 1.7 Å^{-1} in $S(Q)$ diffraction pattern of the glass, but a deeper knowledge of structural packing arrangements of BO_3 and BO_4^- units on the 2−4-Å length scale is required to clarify its origin.

The interpretation of the glassy features as quasi-Bragg scattering related to the presence of large cages in both glassy and equivalent crystalline phases suggests that the parallel decrease of the intensities of the two lowest peak in the static structure factor of $(Cs_2O)_{0.14}(B_2O_3)_{0.86}$, observed when the temperature is raised above 600 K, is due to the forthcoming split.

Moreover, the accommodation of large cesium ions in the larger cages, displacing the oxygens atoms on the boundaries, makes the cages more spherical, reducing the anisotropic disorder and the strain energy and increasing the structural order. This explains the higher degree of order associated with the prominent intensity of the lowest peak and the greater coherence length for it. As the temperature is raised, an increasing degree of roundness is obtained through the relaxation of the residual constraints on the atomic arrangements, and it involves larger distances. Recently, the structural features on the nearest-neighbor length scale were interpreted in terms of a caged cage mechanism related to the arrest in the glassy state.[31] Arrest is characterized by a nonergodicity parameter, $F(Q)$, that describes the degree of arrest at different length scales. Modulation on the length scale beyond the nearest-neighbor shell leads to reduced freezing and smaller $F(Q)$ over a wide Q range. This modulation has a cage-softening effect and weakens the glass, whereas the presence of interstitial particles is expected to strengthen the cages. If the structure in the intermediate length scale below the main peak in $S(Q)$ is implicated in arrest dynamics, relaxations of the atomic arrangements on this length scale are foreseen as a natural result when a thermodynamic parameter (temperature or pressure) is changed.

All of these considerations can be extended to the class of oxide glasses, where a great number of oxygenated structural units building the glassy network form rings of various sizes, and in particular, they can be considered applicable to modified oxide glasses, where the modifier ions are thought to enter the interstices of the network structure. In these systems, the features revealed in the low-Q region of $S(Q)$ should describe the atomic arrangements in large cages. These structures are believed to exist also in their crystalline counterparts, where they are organized in some more ordered fashion. Whether this picture

is appropriate for other glassy systems and hence can provide a unified interpretation of the FSDP in glasses is still to be ascertained.

V. Conclusions

In this article, we present a diffraction study of temperature-induced structural changes in $(Cs_2O)_{0.14}(B_2O_3)_{0.86}$ glass. A length scale for extended-range order was identified. It is associated with the presence of a diffraction peak at $Q_1 = 1.06$ Å^{-1} that precedes the expected FSDP, lying at $Q_2 = 1.74$ Å^{-1} and describing the ordering of B−O-based structural arrangements already present in the B_2O_3 glass. The extended length scale is related to the periodicity arising from the boundaries of the cages that comprise the structure of a three-dimensional network and host the Cs^+ ions. Furthermore, it was observed that, when the temperature was increased to 600K, both the prepeak and the FSDP increased in amplitude and shifted to lower Q values. These findings were ascribed to relaxations of strained arrangements of borate units lying on the boundaries of cages. By annealing the glass at 800 K for a long time, a partially crystalline system was obtained. A good correspondence between the lowest-Q features for glassy and triborate crystalline phases was found, with the peaks in the glass being broadened envelopes of the corresponding peaks of crystalline phase. It was concluded that the essential features of the medium-range structure of $(Cs_2O)_{0.14}(B_2O_3)_{0.86}$ glass can be interpreted on the basis of related crystalline phases.

References and Notes

(1) Sampath, S.; Benmore, C. J.; Lantzky, K. M.; Neuefeind, J.; Leinenweber, K.; Price, D. L.; Yarger, J. L. *Phys. Rev. Lett.* **2003**, *90* (11), 115502. Beaufils, S.; Cormier, L.; Bionducci, M.; Ecolivet, C.; Calas, G.; Le Sauze, A.; Marchand, R. *Phys. Rev. B* **2003**, *67*, 104201. Nakamura, M.; Arai, M.; Inamura, Y.; Otomo, T. *Phys. Rev. B* **2003**, *67*, 064204.

(2) Salmon, P. S.; Martin, R. A.; Mason, P. E.; Cuello, G. J. *Nature (London)* **2005**, *435*, 75.

(3) Sokolov, A. P.; Soltwisch, A.; Quitmann, D. *Phys. Rev. Lett.* **1992**, *69*, 1540.

(4) Leonforte, F.; Boissière, R.; Tanguy, A.; Wittmer, J. P. *Phys. Rev. B* **2005**, *72*, 224206. Monaco, G.; Giordano, V. M. *Proc. Natl. Acad. Sci. U.S.A.* **2009**, *106*, 359.

(5) D'Angelo, G.; Vasi, C.; Bartolotta, A.; Carini, G.; Crupi, C.; Di Marco, G.; Tripodo, G. *Phil. Mag* **2004**, *84*, 1631. Crupi, C.; D'Angelo, G.; Tripodo, G.; Bartolotta, A. *Philos. Mag.* **2007**, *87*, 741.

(6) D'Angelo, G.; Carini, G.; Crupi, C.; Koza, M.; Tripodo, G.; Vasi, C. *Phys. Rev. B* **2009**, *79*, 14206.

(7) Majérus, O.; Cormier, L.; Calas, G.; Beuneu, B. *Chem. Geol.* **2004**, *213*, 89–102.

(8) Busse, L. E.; Nagel, S. R. *Phys. Rev. Lett.* **1981**, *47*, 1848. Busse, L. E. *Phys. Rev. B* **1984**, *29*, 3639.

(9) Tanaka, K. *J. Non-Cryst. Solids* **1987**, *90*, 363. Stone, C. E.; Hannon, A. C.; Ishihara, T.; Kitamura, N.; Shirakawa, Y.; Sinclair, R. N.; Umesaki, N.; Wright, A. C. *J. Non-Cryst. Solids* **2001**, *293*, 769. Inamura, Y.; Katayama, Y.; Utsumiand. Funakoshi, W. *Phys. Rev. Lett.* **2004**, *93* (1), 015501.

(10) Gaskell, P. H.; Wallis, D. J. *Phys. Rev. Lett.* **1996**, *76* (1), 66. Uchino, T.; Harrop, J. D.; Taraskin, S. N.; Elliott, S. R. *Phys. Rev. B* **2005**, *71* (1), 14202.

(11) Allen, D. A.; Howe, R. A.; Wood, N. D.; Howells, W. S. *J. Chem. Phys.* **1991**, *94*, 5071–5076.

(12) Elliott, S. R. *Phys. Rev. B* **1994**, *50*, 5981–5987.

(13) Elliott, S. R. *Europhys. Lett.* **1992**, *19*, 7661.

(14) Chan, S. L.; Elliott, S. R. *Phys. Rev. B* **1991**, *43*, 4423. Beier, W.; Frischat, G. H. *J. Non-Cryst. Solids* **1985**, *73*, 113.

(15) El Alaily, N. A.; Mohamed, R. M. *Nucl. Instrum. Methods Phys. Res. B* **2001**, *179*, 230. Anderson, Yu. E.; Filatov, S. K.; Polyakova, I. G.; Bubnova, R. S. *Glass Phys. Chem.* **2004**, *30*, 450.

(16) Wright, A. C.; Clare, A. G.; Bachra, B.; Sinclair, R. N.; Hannon, A. C.; Vessal, B. *Trans. Am. Crystallogr. Assoc.* **1991**, *27*, 239–253.

(17) Johnson, P. A. V.; Wright, A. C.; Sinclair, R. N. *J. Non-Cryst. Solids* **1982**, *50*, 281.

(18) Armand, P.; Beno, M.; Ellison, A. J. G.; Knapp, G. S.; Price, D. L.; Saboungi, M. L. *Europhys. Lett.* **1995**, *29*, 549.

(19) Price, D. L.; Ellison, A. J. G.; Saboungi, M. L.; Hu, R.-Z.; Egami, T.; Howells, W. S. *Phys. Rev. B* **1997**, *55*, 11249–11255.

(20) Swenson, J.; Börjesson, L.; Howells, W. S. *Phys. Rev. B* **1995**, *52*, 9310.

(21) Hannon, A. C.; Grimley, D. I.; Hulme, R. A.; Wright, A. C.; Sinclair, R. N. *J. Non-Cryst. Solids* **1994**, *177*, 299. Mozzi, R. L.; Warren, J. *Appl. Crystallogr.* **1970**, *3*, 251. Galeener, F. L.; Geissberger, A. E. *J. Phys. (Paris)* **1982**, *C9*, 343. Windisch, C. F., Jr.; Risen, W. M., Jr. *J. Non-Cryst. Solids* **1982**, *48*, 307.

(22) Zhong, J.; Bray, P. J. *J. Non-Cryst. Solids* **1989**, *111*, 67. Meera, B. N.; Ramakrishna, J. *J. Non-Cryst. Solids* **1993**, *159*, 1. Dwivedi, B. P.; Khanna, B. N. *J. Phys. Chem. Solids* **1995**, *56*, 39. Kamitsos, E. I.; Patsis, A. P.; Karakassides, M. A.; Chryssikos, G. D. *J. Non-Cryst. Solids* **1990**, *126*, 52.

(23) Swenson, J.; Börjesson, L.; Howells, W. S. *Phys. Rev. B* **1998**, *57*, 13–514.

(24) González, M. Á.; Mondelli, C.; D'Angelo, G.; Crupi, C.; Johnson, M. R. *J. Non-Cryst. Solids* **2008**, *354*, 203.

(25) Hall, A.; Swenson, J.; Bowron, D. T.; Adams, S. *J. Phys.: Condens. Matter* **2009**, *21*, 245106.

(26) Penin, N.; Touboul, M.; Nowogrocki, G. *Solid State Sci.* **2003**, *5*, 559.

(27) Penin, N.; Seguin, L.; Touboul, M.; Nowogrocki, G. *Solid State Sci.* **2002**, *4*, 67.

(28) Krogh-Moe, J.; Ihara, M. *Acta Crystallogr.* **1967**, *23*, 427. Nowogrocki, G.; Penin, N.; Touboul, M. *Solid State Sci.* **2003**, *5*, 795–803. Penin, N.; Seguin, L.; Touboul, M.; Nowogrocki, G. *J. Solid State Chem.* **2001**, *161*, 205–213.

(29) Krogh-Moe, J. *Acta Crystallogr. B* **1974**, *30*, 1178.

(30) Waclawka, J. *J. Alloys Compd.* **1996**, *244*, 52.

(31) Greenall, M. J.; Voigtmann, Th.; Monthoux, P.; Cates, M. E. *Phys. Rev. E* **2006**, *73*, 050501(R).

JP1005555